Fuel 372 (2024) 132090

Contents lists available at ScienceDirect

Fuel

journal homepage: www.elsevier.com/locate/fuel

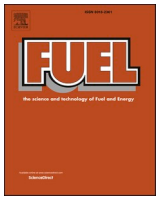

Full Length Article

Optimizing microbial fuel cells with multiple-objectives PSO and type-2 fuzzy neural networks

Mohammad Reza Chalak Qazani [a], Mostafa Ghasemi [b], Houshyar Asadi [c,*]

[a] Faculty of Computing and Information Technology, Sohar University, Sohar, Sohar 311, Oman
[b] Chemical Engineering Section, Faculty of Engineering, Sohar University, Sohar, Sohar 311, Oman
[c] Institute for Intelligent Systems Research and Innovation (IISRI), Deakin University, Geelong, VIC 33216, Australia

ARTICLE INFO

Keywords:
Microbial fuel cell
Clean energy
Type-2 fuzzy neural network
Multiple-objective optimisation
Particle swarm optimisation

ABSTRACT

A microbial fuel cell is a novel method for simultaneous wastewater treatment and electricity production using microorganisms as biocatalysts. This study aims to develop an efficient surrogate model to predict microbial fuel cell performance based on varying input parameters, which include glucose (1–9 g/L), yeast extract (1–5 g/L), and aeration rate (0–110 ml/min). The output parameters of interest are chemical oxygen demand (COD) removal, coulombic efficiency, and power production. A type-2 fuzzy neural network (T2FNN) is employed to train the model for accurate predictions of these outputs. In the second phase, the trained model is integrated with multi-objective particle swarm optimization (PSO) to identify the optimal Pareto front solutions that maximize *COD* removal, coulombic efficiency, and power output. The optimal solutions are validated experimentally, demonstrating a marginal error of 9.50 % between the predicted and observed values. Specifically, the optimized microbial fuel cell achieved a *COD* removal efficiency with a margin error of 7.41 %, a coulombic efficiency margin error of 18.65 %, and a power generation margin error of 2.45 %. Compared to similar studies, the proposed methodology shows significant improvements, highlighting its effectiveness in enhancing microbial fuel cell performance for bioelectricity production and wastewater treatment. On average, the optimal parameters identified using this method result in notable improvements in *COD* removal, coulombic efficiency, and power production compared to a full factorial experimental study.

1. Introduction

The two big challenges of the world are supplying clean water and energy. Water scarcity and global warming are threats to human life globally. With the rapid population growth of the world and living standards, pressure on the existing water and energy sources has jumped up [1–3]. Also, world capitalism has increased the resource usage. The rapid population growth needed to approach the economic government's vision results from the current situation. The statistics predict that in less than 50 years, about 30 % of the people will have no access to water and about 1 billion people, which means 13 % of the population, will have no electricity [4–6]. The critical and high demand for a new energy source made all the governments think about alternative energy sources that don't pollute the environment, have no environmental effect, and are renewable. The microbial fuel cell is a device that can reduce the pollution of the environment, reduce carbon dioxide release, and treat wastewater. It also produces electricity as clean fuel by using microorganisms, and the fuel of the microbial fuel cell is free. It is also an efficient machine for extracting energy from the substrates in wastewater, such as carbon and nitrogen [7–9].

Furthermore, microbial fuel cells can produce clean, renewable fuel and reduce the hazardous carbon effect. Microbial fuel cells need less energy compared to other techniques for wastewater treatment. The removal of chemical oxygen demand in a microbial fuel cell is the oxidation of organic materials in the substances by using electroactive bacteria [10,11]. This results in a transfer of the protons and electrons to the electrode as an electron acceptor. Microbial fuel cells collect electricity by applying several microorganisms for electrochemical reactions. Microorganisms that generate a layer on the anode can move electrons to the anode and then by bacterial pili or nanowires. The performance of a microbial fuel cell depends on different parameters such as electrode, separator and cathode catalyst. Beyond all these parameters, the media is the fuel and feed of microorganisms, such as the engine and biocatalyst in bioelectricity generation and wastewater treatment [12].

* Corresponding author.
E-mail address: houshyar.asadi@deakin.edu.au (H. Asadi).

https://doi.org/10.1016/j.fuel.2024.132090
Received 22 April 2024; Received in revised form 29 May 2024; Accepted 31 May 2024
Available online 14 June 2024

Nomenclature

Symbols

CC	Correlation coefficient
COD	Chemical oxygen demand
FFNN	Feedforward neural networks
FIS	Fuzzy inference system
GA	Genetic algorithm
MSE	Mean square error
ORR	Oxygen reduction reaction
PSO	Particle swarm optimization
RMSE	Root mean square error
SVR	Support vector regression
T2FNN	Type-2 fuzzy neural network

Acronyms

a_i	Type-2 FIS IF-THEN rule
b	Number of transferred electrons per mole of oxygen
C_1	Individual confidence factor
C_2	Swarm confidence factor
F	Faraday number
I	Current
$\max_{gen}$	Maximum number of generations
$\max_{vel}$	Maximum vel in percentage
M	Molecular weight of oxygen
N_p	Population size
N_r	Repository size
$n_{grid} = 20$	Number of grids in each dimension
n_{x_i}	Corresponding normalised data
P	Power
$\boldsymbol{Q}_{\boldsymbol{u}}^{a}$	Comprise sets of type-2 FISs
$\boldsymbol{Q}_{\boldsymbol{v}}^{a}$	Comprise sets of type-2 FISs
R	External resistance
$\boldsymbol{u}_i^*$	Reference signals with a_i
u_{mut}	Uniform mutation percentage
V	Voltage
V_{an}	Volume of the anode chamber
$\boldsymbol{v}_i^*$	Reference signals with a_i
W	Inertia weight
$\overline{x}$	Maximum values of the dataset
$\underline{x}$	Minimum values of the dataset
x_i	Raw data at the i^{th} position
$\underline{\mu}_{\boldsymbol{x}_i}^{a}$	Minimum outputs of the fuzzy rules
$\overline{\mu}_{\boldsymbol{x}_i}^{a}$	Maximum output of the fuzzy rules

Soft computing techniques have recently emerged in various domains, such as materials microstructure, manufacturing, and energy production [13–15]. Fang *et al.* [16] introduced an integrated modelling approach combining uniform design, relevance vector machine, and accelerating genetic algorithm to optimize microbial fuel cell performance, achieving high Coulombic efficiency and power density under optimal conditions. Garg *et al.* [17] explored multi-gene genetic programming, feedforward neural networks (FFNN), and support vector regression (SVR) to model microbial fuel cell performance, attempting to predict pre-and post-startup microbial fuel cell voltage based on temperature and ferrous sulphate concentrations. However, their model proved time-consuming and unsuitable for real-time applications. Chen *et al.* [18] introduced a hybrid soft computing model featuring wavelet analysis, ELM, and genetic algorithms (GA) to evaluate the influence of factors like relative humidity, load current, hydrogen pressure, and temperature on proton exchange in microbial fuel cells designed for electric vehicles. Although experimental results demonstrated the efficacy of their approach compared to traditional methods like Elman and relevance vector machines, practical implementation remains a challenge. Cai *et al.* [19] demonstrated that incorporating microbial community data with six machine-learning algorithms can accurately predict feed substrates in microbial fuel cells, achieving high accuracies (over 93 %) and enhancing microbial fuel cell-based biosensor signal specificity. Yewale *et al.* [20] developed a temperature-based mathematical model and a multiple models-based control strategy using various machine learning approaches, achieving a 65 % reduction in average settling time for controlling continuous microbial fuel cells. Dwivedi et al. [21] conducted a comprehensive review of the current research in microbial fuel cells, focusing on integrating soft computing methods to enhance the performance of these environmentally friendly applications. Jadhav *et al.* [22] explored various mathematical and computational modelling strategies to optimize microbial fuel cell performance, highlighting the importance of model-based optimization and process control for scaling up and commercializing microbial fuel cell technology. Additionally, Nguyen et al. [23] introduced a deep learning approach that combines multi-layer perceptron and GA to develop a three-dimensional Multiphysics model for microfluidic microbial fuel cells.

Ghasemi et al. [24] used a multi-layer perceptron with varying hidden layers to significantly enhance the accuracy of predicting microbial fuel cell performance, demonstrating a 5.1819-fold improvement compared to the traditional SVR method. In addition, Ghasemi et al. [25] utilised fuzzy modelling and the salp swarm optimizer to enhance microbial fuel cell performance, achieving simultaneous improvements in power density, *COD* removal, and coulombic efficiency. Abdollahfard *et al.* [26] enhanced microbial fuel cell performance by using random forest and gradient boost regression models to predict power density and *COD* removal, optimized via particle swarm optimization, identifying key parameters for maximization. Nguyen *et al.* [27] introduced explainable artificial intelligence to analyse machine learning models for optimizing membrane less microbial fuel cells, achieving a 239.024 % increase in power density and offering valuable insights into key operating parameters. Hossain *et al.* [28] introduced Bayesian optimization-SVR and Bayesian optimization-Boosted Regression Tree super learner models for predicting microbial fuel cell power generation, demonstrating that BA-SVR significantly outperforms existing models in accuracy and robustness, thus optimizing electricity estimation and reducing laboratory trials. Recently, Kebede *et al.* [29] proposed a transfer learning approach using a variational autoencoder and Bi-LSTM with an attention mechanism for predicting remaining useful life of microbial fuel cells, achieving superior accuracy and efficiency in stack voltage degradation estimation. Li *et al.* [30] presented an integrated framework using multi-physics models, machine learning (AdaBoost), and an enhanced grey wolf optimizer to swiftly optimize channel structure, maximizing power density with high accuracy and efficiency.

However, despite these advancements, several gaps remain in the literature:

1. Limited Integration of Type-2 Fuzzy Neural Networks (T2FNN): Previous studies have predominantly used traditional neural networks and machine learning techniques. The application of T2FNNs, which can handle higher levels of uncertainty and imprecision in data, is still underexplored in the context of microbial fuel cell optimization.
2. Comprehensive Multi-Objective Optimization: While some studies have addressed single-objective optimization, there is a lack of comprehensive approaches that simultaneously optimize multiple

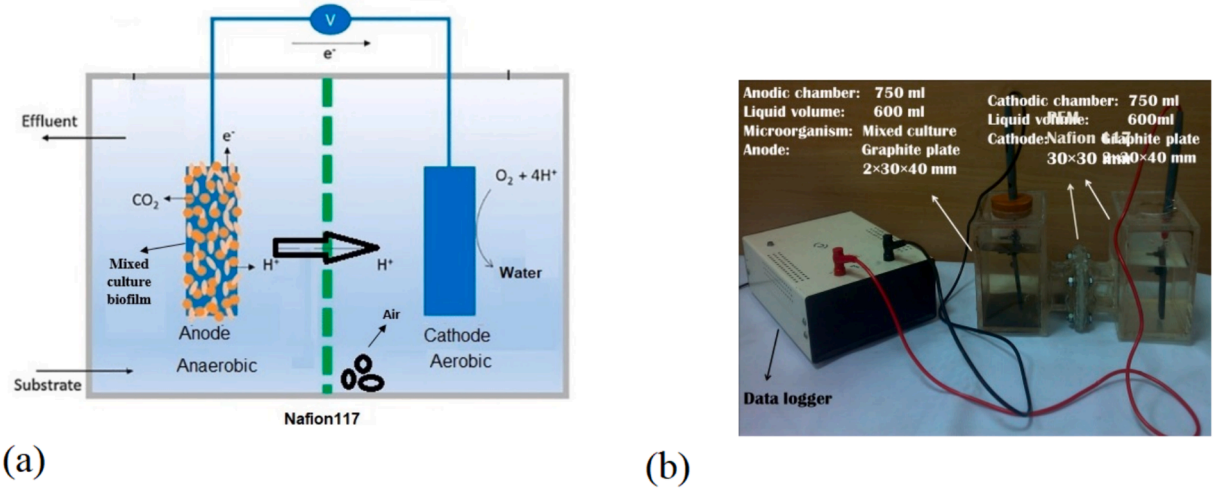

Fig. 1. (a): The schematic of a microbial fuel cell; (b): The experiment setup for capturing the *COD* removal, coulombic efficiency, and power generation based on glucose, yeast extract, and aeration.

critical outputs like *COD* removal, coulombic efficiency, and power density.

3. Experimental Validation of Soft Computing Models: Many studies present computational models without sufficient experimental validation, leaving a gap in confirming these models' practical applicability and accuracy in real-world settings.

The main motivation of the current study can be categorised into two different points. Initially, the surrogate model was developed to imitate the microbial fuel cell's behaviour in calculating the chemical oxygen demand (*COD*) removal, coulombic efficiency, and power based on glucose, yeast extract, and aeration as operation parameters. Also, extracting the optimal solution of the input parameters results in the system's maximum performance. Then, the study's main contribution lies in developing and applying a novel methodology that combines T2FNN with multiple-objective particle swarm optimization (PSO) to optimise the performance of a microbial fuel cell process by choosing the optimized media through a new method. The methodology begins with a comprehensive experimental investigation, using a full factorial design to analyse the impact of various input process parameters on key outcomes, including *COD* removal, coulombic efficiency, and power. Subsequently, three distinct T2FNN models are developed to predict these outcomes accurately. The main motivation for selecting T2FNN in comparison to other machine learning methods:

1. Handling Uncertainty: T2FNNs are designed to manage and model the uncertainty and imprecision inherent in real-world data more effectively than traditional ANNs. This is particularly important in biological systems like microbial fuel cells, where data variability is high.
2. Higher Accuracy and Robustness: T2FNNs provide better accuracy and robustness in predicting outputs, accounting for a wider range of input variations and uncertainties.
3. Flexibility and Modularity: Using separate T2FNNs for each output allows for greater flexibility and modularity in system design, making it easier to update or refine individual models as needed without affecting the entire system.

By using three separate T2FNNs, this study ensures higher accuracy, simplicity, lower computational load, and better applicability, thereby addressing the critical needs of microbial fuel cell optimization more effectively than a single ANN model with multiple outputs. It should be noted that the results of the developed T2FNN models are compared with traditional machine learning models, including decision tree (DT), SVR, and FFNN, to prove the higher efficiency of the proposed method in this research.

These T2FNN models are integrated into a multiple-objectives PSO framework, where the objective functions are based on mean square error between experimental and predicted values. The optimization process aims to maximize *COD* removal, coulombic efficiency, and power generation in the microbial fuel cell process. This study provides a systematic approach to optimize microbial fuel cell performance, which can have significant implications for various biotechnology and renewable energy applications. This study is the first time the media in the microbial fuel cell was optimized using the T2FNN method, and the model was validated.

Section 2 comprehensively examines the microbial fuel cell process, specifically defining the inputs and capturing the system's outputs. Furthermore, this Section outlines the methodology for acquiring the necessary datasets and utilizing the experimental study. Moving forward to Section 3, a detailed explanation regarding the innovative approach incorporating the combined utilization of T2FNN and multiple-objectives PSO is provided. Section 4 of this manuscript offers a comprehensive comparative analysis and thought-provoking discussion, delving into the outcomes extracted through the developed model implemented within the MATLAB framework. Finally, in Section 5, the study reaches its culmination as key conclusions derived from the research are summarized and highlighted.

2. Materials and methods

2.1. Microbial fuel cell configuration

The microbial fuel cell structure is similar to our previous study [31]. The microbial fuel cell is built by two chambers that have been separated by a separator, which is a proton exchange membrane (Nafion117). Nafion 117 has high selectivity; only protons can pass through that and reach the anode. The electricity is generated by the oxygen reduction reaction (ORR) reaction on the surface of the cathode electrode, and the voltage is recorded on a PC. The schematic diagram of a microbial fuel cell is shown in the Fig. 1a. Carbon paper was used as the electrode in anode and carbon paper/Pt in employed as the cathode electrode.

2.2. Media and inoculation

Different concentrations of glucose (1–9 g/l) are used as carbon sources. The yeast extract in variable amounts was used as a nitrogen source (1–5 g/l). Mineral and vitamin components were used as

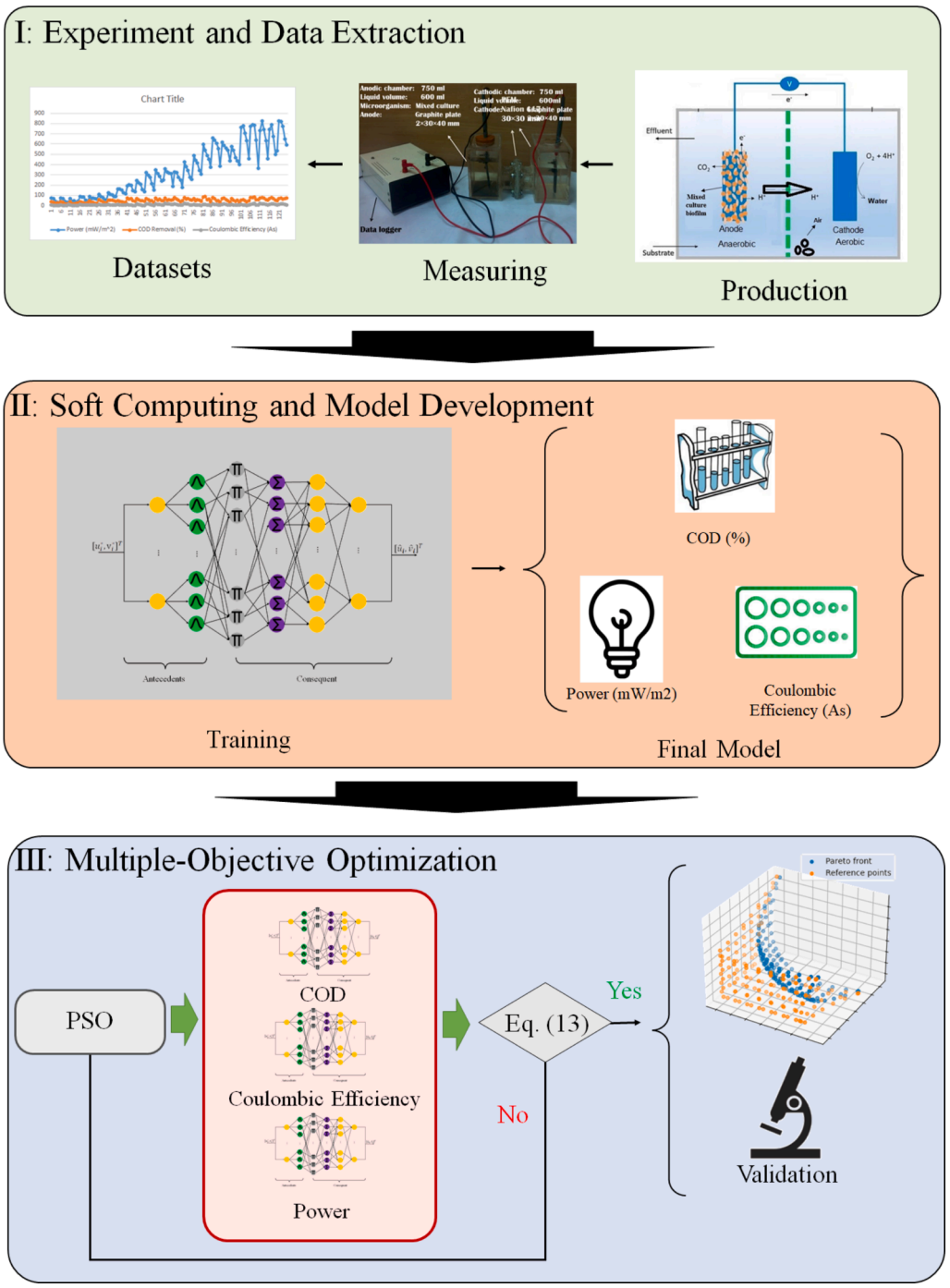

Fig. 2. The proposed research methodology's graphical abstract for extracting the optimal microbial fuel cell parameters.

described before. Also, the nitrogen was purged in the anode chamber for 15 min before the start of the experiment to make the anode anaerobic. Also, the air is purged by an aquarium pump to the cathode chamber for ORR reaction.

The media was inoculated by palm oil mill effluent (POME, Selangor) as an anaerobic sludge in an anaerobic beaker. Before the operation, 10 ml of the sludge has been added to the media. The attached microorganisms were observed by scanning electronic microscopy (SEM-Surpra-55vp-Zeiss, Germany). The samples were dried and covered by a thin layer of gold before the photo was captured. Fig. 1b shows the experimental setup for holding the experiment to capture the *COD* removal, coulombic efficiency, and power generation based on glucose, yeast extract, and aeration. To start the operation, 10 ml of the sludge has been added to the media in the anode chamber of microbial fuel cell. Then the MFC is connected to the voltameter and fed every 90 h. It took about three weeks that the voltage of MFC get stable. Then the resistances were connected to the MFC for producing the current.

2.3. Analysis and calculation

A voltammeter measures the produced voltage in each second and is recorded and saved on a PC. The current and voltage produced can be calculated using the formula below.

$$I = \frac{V}{R} \tag{1}$$

Table 1
Different levels of the input parameters for the design of the experiment.

Parameters	L1	L2	L3	L4	L5
Glucose (g/L)	1	3	5	7	9
Yeast Extract (g/L)	1	2	3	4	5
Aeration (mL/min)	0	20	50	80	110

$$P = V \times I \tag{2}$$

where the current is noted as I and the voltage is noted as V. The external resistance is shown as R.

The *COD* reagents (high range) were used to measure the *COD*. A sample was taken from the anode chamber to find the *COD* and then diluted 10-fold in water. Then, 2 mL of the sample was added to the high-range *COD* vials and heated to150 ^{o}C. Finally, a spectrophotometer was used to measure *COD* [32].

This formula can calculate the system's coulombic efficiency as follows:

$$CE = \frac{M \int_0^t I dt}{FbV_{an}\Delta COD} \tag{3}$$

where M is the molecular weight of oxygen, and F is the Faraday number. The number of transferred electrons per mole of oxygen is $b = 4$. The change of *COD* is shown by ΔCOD and V_{an} is the volume of the anode chamber. Nitrogen gas was purged inside the anode chamber for 10 min to provide the anaerobic condition. From the other side, the air was continuously purged in the cathode chamber for the ORR reaction.

3. Simulation method

This Section's focal point lies in the proposed methodology, which revolves around developing T2FNN. Fig. 2 shows the graphical abstract of the proposed methodology in this research. It consists of three main steps, including extracting the dataset using practical experiments, developing T2FNN as a representative of soft computing method, and extracting optimal processing parameters using multiple-objectives PSO.

The first step comprises three sub-steps, including the production of microbial fuel cells using different input parameters (glucose, yeast Extract, and aeration). A comprehensive investigation employs a full factorial microbial fuel cell process analysis. This study embraces the fully experimental study to capture the different outcomes of the process, including *COD* removal, coulombic efficiency, and power. To reach the system's highest possible accuracy, the experiment's full factorial design is investigated using the different levels for each input process parameter, as shown in Table 1. The dataset comprises 125 samples related to different experimental setups for each scenario. The extracted dataset is reported in the supplementary file as a.csv file.

The second step entails the utilisation of T2FNN to derive a surrogate model that faithfully emulates the behaviour exhibited by the microbial fuel cell process. The extracted dataset is divided into 70 % and 30 % for training and testing purposes of the proposed T2FNN. It should be noted that for the sake of simplicity, lower computational load, and applicability, three T2FNNs are proposed to calculate the *COD* removal, coulombic efficiency, and power, which is called COD-T2FNN, CE-T2FNN, and P-T2FNN, respectively. The influence of different input parameters can be evaluated on the outcomes of the microbial fuel cell process.

In the third step, these three extracted T2FNN models are employed inside multiple-objectives PSO as three separate cost functions to extract the optimal Pareto front solutions. After extracting these optimal Pareto solutions, the extracted optimal parameters are validated using the real experiment to prove the higher efficiency of the proposed method in real-life applications.

3.1. Preprocessing

The raw datasets cannot be directly fed into the algorithm, which would compromise the model's accuracy. Hence, we delve into the importance of data preprocessing. The dataset undergoes a crucial preprocessing stage to enhance the network's accuracy, aimed at mitigating the system's complexity. The process commences by removing out-of-range data, as these entries significantly impede the network's precision. Subsequently, normalisation takes centre stage, facilitating the allocation of mean and standard deviation values within a rational range. By achieving this, the system's complexity is effectively reduced, streamlining the network's operations. The calculations involved in this normalisation process are as follows:

$$n_{x_i} = \frac{x_i - \underline{x}}{\overline{x} - \underline{x}} \tag{4}$$

where $\overline{x}$ and $\underline{x}$ are the maximum and minimum values of the dataset. Additionally, let x_i represent the raw data at the ith position while n_{x_i} symbolises the corresponding normalised data. The normalised values are constrained within the interval [0,1]. Acknowledging that the normalisation procedure is conducted independently for input and output data is vital.

Concluding the data preprocessing stage involves partitioning the dataset into distinct training and testing samples. For this study, 70 % of the dataset is allocated for training. The remaining 30 % is reserved for testing the network's performance.

3.2. Type-2 fuzzy neural network

T2FNN emerges as a powerful fusion, integrating a neural network and a type-2 fuzzy inference system (FIS) to achieve optimal tuning. The type-2 FIS takes centre stage within this study, meticulously calculating

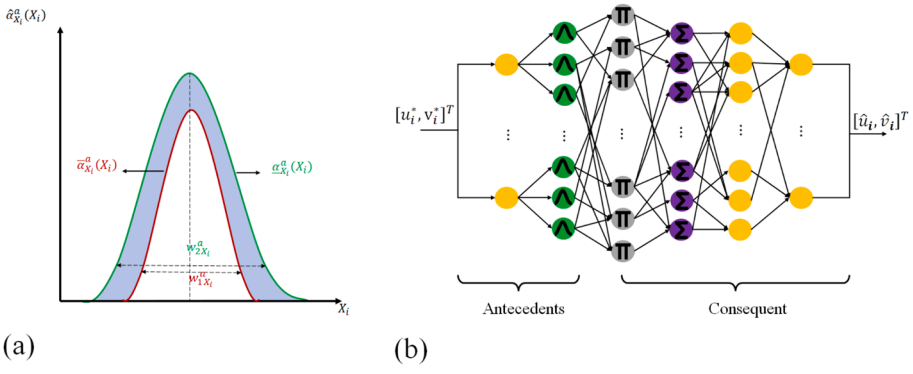

Fig. 3. (a): Membership function of the type-2 fuzzy interface; (b): Schematic representation of the T2FNN.

COD removal, coulombic efficiency, and power in the microbial fuel cell process. These components, denoted as COD-T2FNN, CE-T2FNN and P-T2FNN, deliver accurate insights. Fig. 3a artistically showcases the membership functions employed by the interval type-2 FIS. These functions have been strategically designed to handle the intricacies of *COD* removal, coulombic efficiency, and power.

Moreover, complementing the type-2 FIS model, an FFNN has been seamlessly integrated. It helps to predict *COD* removal, coulombic efficiency, and power more accurately. The comprehensive structure of this hybrid T2FNN model is skilfully depicted in the captivating Fig. 3b.

The T2FNN involves the development of the considered system through the utilisation of multiple type-2 FIS IF-THEN rules, as outlined below [33]:

Rule a_i : IF $u_i^* \in \boldsymbol{Q}_{\boldsymbol{u}}^a$ and $v_i^* \in \boldsymbol{Q}_{\boldsymbol{v}}^a$

$$\text{THEN}: \ \boldsymbol{X}_i^a = \begin{bmatrix} (u_i^a)^T & (v_i^a)^T \end{bmatrix} = \widehat{r}_{i0}^a + \widehat{\boldsymbol{R}}_{i0}^a \begin{bmatrix} (u_i^*)^T & (v_i^*)^T \end{bmatrix}^T = \widehat{r}_{i0}^a + \widehat{\boldsymbol{R}}_{\boldsymbol{u},\boldsymbol{v}}^a \boldsymbol{X}_i^* \tag{5}$$

where:

$$\widehat{\boldsymbol{R}}_{\boldsymbol{u},\boldsymbol{v}}^a = \begin{bmatrix} \widehat{r}_{\boldsymbol{u},\boldsymbol{v},1}^a & \cdots & \widehat{r}_{\boldsymbol{u},\boldsymbol{v},5}^a \end{bmatrix} \quad \textbf{\textit{while}} \quad \widehat{r}_{\boldsymbol{u},\boldsymbol{v},n}^a \in \begin{bmatrix} \underline{r}_{\boldsymbol{u},\boldsymbol{v},n}^a & \overline{r}_{\boldsymbol{u},\boldsymbol{v},n}^a \end{bmatrix}, \ n = 1, \ldots, 5 \tag{6}$$

Moreover, $\boldsymbol{u}_i^*$ and $\boldsymbol{v}_i^*$ represent the reference signals with a_i denoting the number of rules for systems i within the set $\{n, q\}$. Additionally, $\boldsymbol{Q}_{\boldsymbol{u}}^a$ and $\boldsymbol{Q}_{\boldsymbol{v}}^a$ comprise sets of type-2 FISs, each equipped with their respective membership functions.

Therefore:

$$\underline{\boldsymbol{X}}_i^a = \underline{r}_{i0}^a + \underline{\boldsymbol{R}}_{\boldsymbol{u},\boldsymbol{v}}^a \boldsymbol{X}_i^*$$

$$\overline{\boldsymbol{X}}_i^a = \overline{r}_{i0}^a + \overline{\boldsymbol{R}}_{\boldsymbol{u},\boldsymbol{v}}^a \boldsymbol{X}_i^* \tag{7}$$

Using the fuzzy sets illustrated in Fig. 3a as a reference, we define $\widehat{\alpha}_{\boldsymbol{u}}^a(\boldsymbol{v}_i) = \left[\underline{\alpha}_{\boldsymbol{u}}^a(\boldsymbol{v}_i), \overline{\alpha}_{\boldsymbol{u}}^a(\boldsymbol{v}_i)\right]$ and $\widehat{\alpha}_{\boldsymbol{u}}^a(\boldsymbol{u}_i) = \left[\underline{\alpha}_{\boldsymbol{u}}^a(\boldsymbol{u}_i), \overline{\alpha}_{\boldsymbol{u}}^a(\boldsymbol{u}_i)\right]$ as uncertain standard deviation and mean Gaussian functions, while [34]:

$$0 \leqslant \underline{\alpha}_{\boldsymbol{X}_i}^a(\boldsymbol{X}_i) \leqslant \overline{\alpha}_{\boldsymbol{X}_i}^a(\boldsymbol{X}_i) \leqslant 1 \tag{8}$$

and

$$\underline{\alpha}_{\boldsymbol{X}_i}^a(\boldsymbol{X}_i) = e^{\left(-\frac{1}{2}\left(\frac{X_i - c_{X_i}^a}{w_{1X_i}^a}\right)^2\right)}$$

$$\overline{\alpha}_{\boldsymbol{X}_i}^a(\boldsymbol{X}_i) = e^{\left(-\frac{1}{2}\left(\frac{X_i - c_{X_i}^a}{w_{2X_i}^a}\right)^2\right)} \tag{9}$$

By multiplying the type-2 fuzzy sets, the final outputs of the fuzzy rules in each system are determined in the following manner:

$$\underline{\mu}_{\boldsymbol{X}_i}^a(\boldsymbol{X}_i) = \underline{\alpha}_{\boldsymbol{u}}^a(\boldsymbol{u}_i) \times \underline{\alpha}_{\boldsymbol{u}}^a(\boldsymbol{v}_i)$$

$$\overline{\mu}_{\boldsymbol{X}_i}^a(\boldsymbol{X}_i) = \overline{\alpha}_{\boldsymbol{u}}^a(\boldsymbol{u}_i) \times \overline{\alpha}_{\boldsymbol{u}}^a(\boldsymbol{v}_i) \tag{10}$$

So:

$$\widehat{X}_i = \frac{1}{2}\left(\frac{\sum_{a=1}^{A_i} \underline{\mu}_{X_i}^a(X_i) \underline{X}_i^a}{\sum_{a=1}^{A_i} \underline{\mu}_{X_i}^a(X_i)} + \frac{\sum_{a=1}^{A_i} \overline{\mu}_{X_i}^a(X_i) \overline{X}_i^a}{\sum_{a=1}^{A_i} \overline{\mu}_{X_i}^a(X_i)}\right) \tag{11}$$

The generation of parameters within the type-2 FIS is accomplished by training a neural network utilising the datasets employed in this study. The fuzzy neural network, operating on the principles of the Takagi-Sugeno fuzzy structure, skilfully incorporates the represented rules outlined in Eq. (6). Visualising the intricate mechanism of the T2FNN is Fig. 3b, a captivating depiction illustrating the system's functionality through the arrangement of five layers or two distinct main groups, namely the antecedents and the consequents.

Three parameters have been used to validate our investigated methods to choose the most reliable one, including correlation coefficient (CC), mean square error (MSE), and root mean square error (RMSE). These validation parameters are calculated as follows:

$$CC = \frac{\sum_{i=1}^{n}((x_i - \overline{x})(T_i - \overline{T}))}{\sqrt{\sum_{i=1}^{n}\left((x_i - \overline{x})^2 (T_i - \overline{T})^2\right)}}$$

$$MSE = \frac{1}{n}\sum_{i=1}^{n}(T_i - \widehat{T}_i)^2$$

$$RMSE = \sqrt{\frac{\sum_{i=1}^{n}(T_i - \widehat{T}_i)^2}{n}} \tag{12}$$

where n, x_i, and $\overline{x}$ are the number of samples, the i^{th} input, and the mean of inputs.

3.3. Multiple-objectives particle swarm optimisation

PSO has been widely used for optimisation problems since its proposal by Kennedy and Eberhart in 1997 [35]. An extended version called multiple-objectives PSO was introduced by Coello *et al.* in 2004 [36] to address multiple-objectives optimisation problems. Multiple-objectives PSO incorporates an external repository, consisting of an archive controller and an adaptive grid, to store the non-dominated solutions discovered during the search process.

The archive controller determines whether a new solution should be added to or removed from the archive. In comparison, the adaptive grid aims to distribute the objective function space uniformly by dividing it into regions. In contrast, traditional methods convert multiple-objectives into a single objective. Multiple-objectives PSO directly handles multiple-objectives optimisation problems without needing multiple runs and achieves more accurate results, especially for disjointed and concave Pareto fronts. However, in multiple-objectives optimisation problems, multiple global optima exist along the Pareto front. Therefore, multiple-objectives PSO maintains a repository of nondominated particles and employs the adaptive grid method to assign each particle a leader from the repository. This approach ensures a diverse and accurate approximation of the Pareto front. Within this study, three objective functions are determined through the calculation of the mean square error (MSE) between the actual values acquired via experimental study and the predictions generated by the proposed T2FNN models:

$$J_{COE}(G, YE, A) = 100 - \frac{1}{n}\sum_{i=1}^{n}(COD_i - \widehat{COD}_i)^2$$

$$J_{CE}(G, YE, A) = 500 - \frac{1}{n}\sum_{i=1}^{n}(CE_i - \widehat{CE}_i)^2$$

$$J_P(G, YE, A) = 1000 - \frac{1}{n}\sum_{i=1}^{n}(P_i - \widehat{P}_i)^2 \tag{13}$$

where G, YE, and A are glucose, yeast extract, and aeration, respectively. In addition, *COD*, *CE*, and *P* stand for actual *COD* removal, coulombic efficiency, and power, respectively. It should be noted that the $\widehat{COD}$, $\widehat{CE}$, and $\widehat{P}$ are predicted *COD* removal, coulombic efficiency, and power by COD-T2FNN, CE-T2FNN, and P-T2FNN models, respectively. It should be noted that the best solution for the microbial fuel cell process is the generation of higher *COD* removal, coulombic efficiency, and power. Then, the constant parameters 100, 50, and 1000 are defined inside Eq. (13) to extract the system's maximum regenerated outputs during

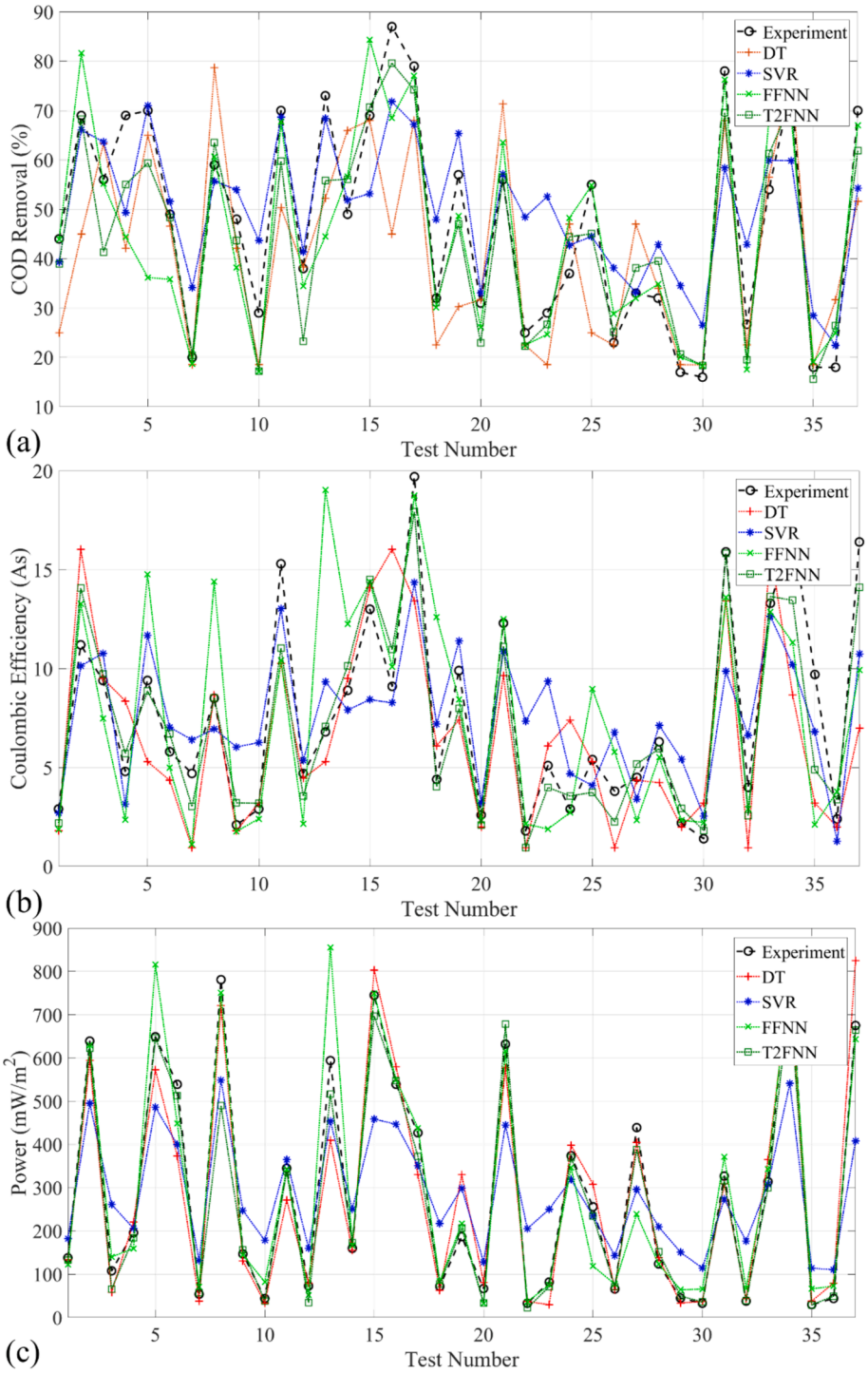

Fig. 4. The experimental and predicted outputs of microbial fuel cell process using DT, SVR, FFNN, and T2FNN for calculation of (a) *COD* removal (%); (b) coulombic efficiency (As); (c) power (mW/m^2).

optimisation.

In this research, the provided platform in MATLAB by Víctor Martínez-Cagigal [37] is employed to extract the 3-dimensional Pareto front distribution of the optimal microbial fuel cell process parameters. The hyperparameters of the investigated multi-objective PSO were chosen through a trial-and-error approach to achieve the minimum cost function as described in Eq. (13). This approach was taken to ensure that the algorithm could effectively explore and exploit the solution space for optimal performance. The selected hyperparameters are $N_p = 20$, $N_r = 200$, $\max_{gen} = 100$, $W = 0.4$, $C_1 = 2$, $C_2 = 2$, $n_{grid} = 20$, $\max_{vel} = 5$, $u_{mut} = 0.5$. These values were iteratively adjusted based on their impact on the convergence and diversity of the solutions. The chosen parameters reflect a balance between computational efficiency and the thoroughness of the search process, ensuring that the PSO algorithm can effectively find and refine the Pareto-optimal solutions for maximizing COD removal, coulombic efficiency, and power generation.

4. Results and discussions

This Section is composed of four subsections. The first subsection

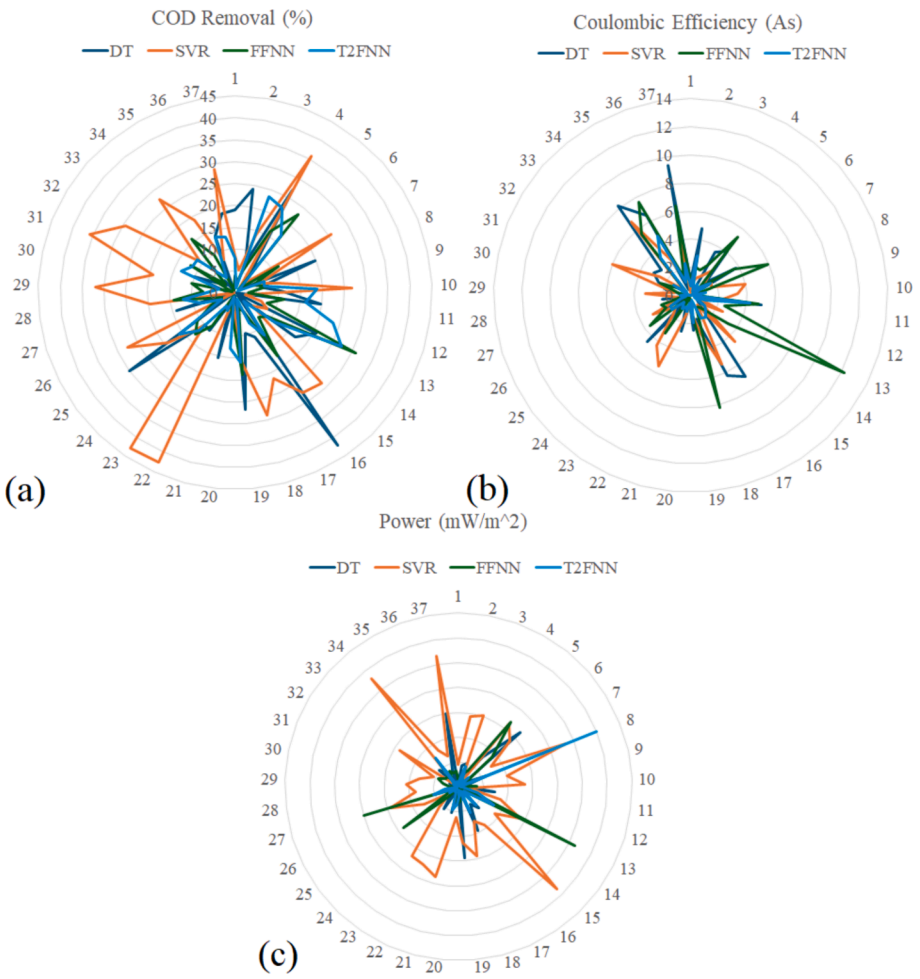

Fig. 5. The error between the experimentally captured and predicted value using the four investigated models, including DT, SVR, FFNN, and T2FNN, to predict (a) *COD* removal (%); (b) coulombic efficiency (As); (c): power (mW/m^2).

focuses on developing T2FNN modelling of the system to extract the most reliable models to calculate the *COD* removal, coulombic efficiency, and power based on glucose, yeast extract, and aeration. Traditional machine learning methods, including DT, SVR, and FFNN, have also been designed and developed to validate the newly proposed T2FNN in terms of accuracy and efficiency. In the second subsection, the influence of the input parameters (glucose, yeast extract, and aeration) on the variation of output parameters (*COD* removal, coulombic efficiency, and power) are analysed based on the extracted efficient T2FNN models. In the fourth subsection, the most accurate extracted T2FNN models in calculating *COD* removal, coulombic efficiency, and power are employed inside the multiple-objectives' optimisation (based on Section 3.3) to extract the optimal solution of the operation to maximise the outputs of the system. At last, the extracted optimal solutions via multiple-objectives PSO are experimentally validated to prove the efficiency of the proposed method.

4.1. Modelling and evaluation

In the first step of the implementation process, four different methods are designed and developed under MATLAB software to prove the higher efficiency of the proposed T2FNN in terms of higher accuracy and lower computational load. DT, SVR, and FFNN are developed using fitrtree, fitrsvm, and feedforwardnet, respectively. In addition, T2FNN is designed and developed based on the represented model in Section 3.2. 70 % and 30 % of the extracted dataset during the experiment in Section 2 are used for training and testing purposes of the four investigated methods, respectively.

Fig. 4a–c displays *COD* removal, coulombic efficiency, and power assessment within the microbial fuel cell process using experiment, DT, SVR, FFNN and T2FNN during the testing process of the models. This appraisal involves employing the network's testing phase, as the network's accuracy during the testing process is more critical for engineering applications. The experimental results are the benchmark against which the outcomes of the other three methods are calculated, facilitating an evaluation of the proposed models' precision. Fig. 4a delineates the computation of *COD* removal for 37 testing samples, utilizing both the experiment and *COD* removal calculation via DT, SVR, FFNN, and T2FNN. As evidenced by the findings in Fig. 4a, the CC between the experimental outcomes and the extracted *COD* removal yielded by the DT, SVR, FFNN, and T2FNN amounts to 0.7561, 0.7658, 0.8648, and 0.9412, respectively. It proves the higher efficiency of our newly proposed T2FNN in the prediction of *COD* removal by improving the accuracy of the network by 24.48 %, 9.48 %, and 8.83 %, compared with those of DT, SVR, and FFNN, respectively, in term of CC. Furthermore, Fig. 4b demonstrates that encompassing 37 testing samples, the CC between the experimental results and the extracted coulombic efficiency generated by the suggested DT, SVR, FFNN, and T2FNN models stands at 0.7451, 0.7868, 0.7343, and 0.9453, respectively. It proves the higher efficiency of our newly proposed T2FNN in the prediction of *COD* removal by improving the accuracy of the network by 26.87 %, 16.10 %, and 28.73 %, compared with those of DT, SVR, and FFNN, respectively, in term of CC. Also, the CC between the experimental results and the extracted power by the DT, SVR, FFNN, and T2FNN models are 0.9677,

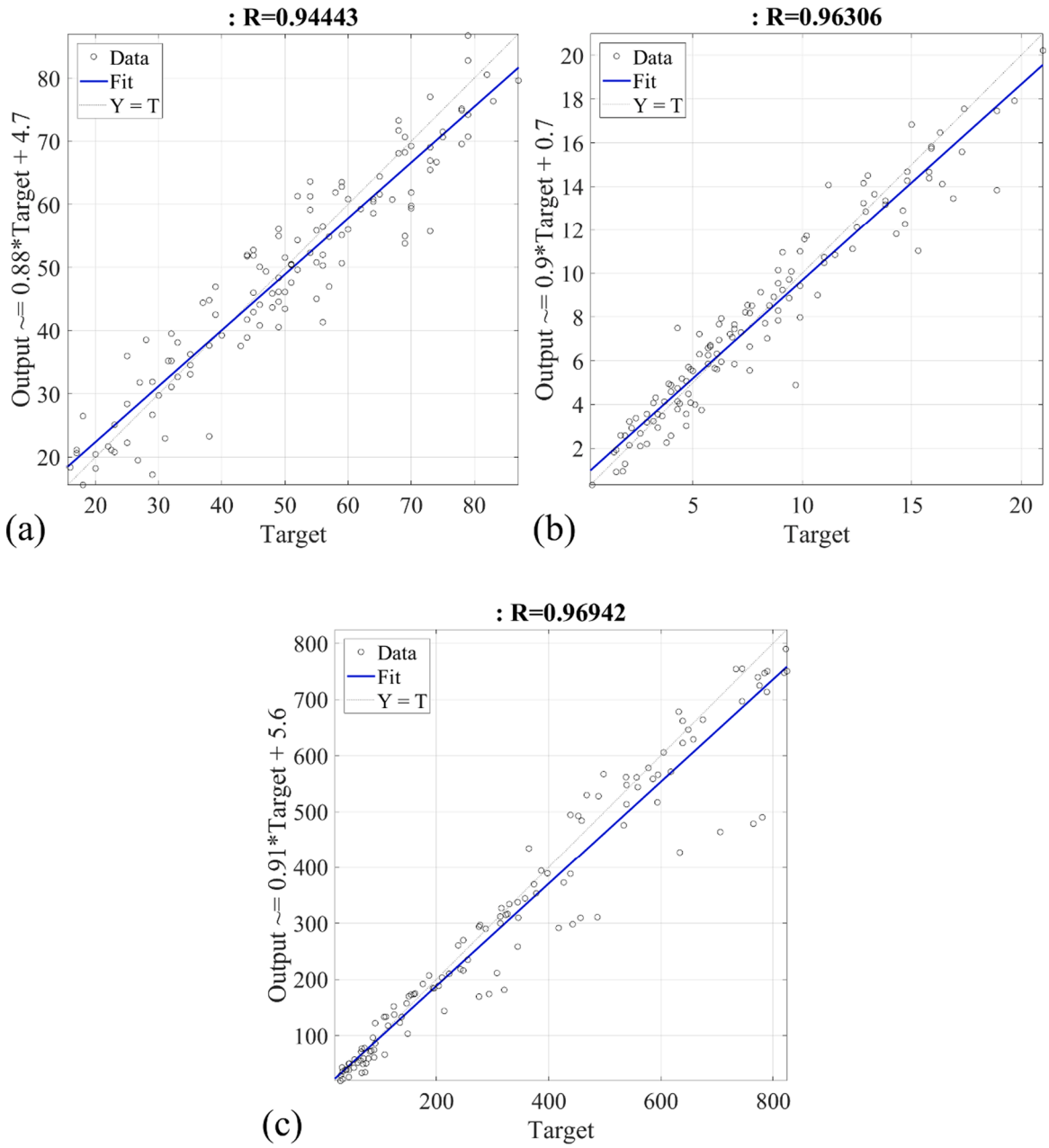

Fig. 6. The regression of the whole dataset (training and testing) using (a) COD-T2FNN for prediction of the *COD* removal (%); (b) CE-T2FNN for prediction of the coulombic efficiency (As); (c) P-T2FNN for prediction of the power (mW/m^2).

0.9462, 0.9643, and 0.9804 based on the represented results in Fig. 4c. It proves the higher efficiency of our newly proposed T2FNN in prediction of *COD* removal by improving the accuracy of the network by 1.31 %, 2.51 %, and 1.67 %, compared with those of DT, SVR, and FFNN, respectively, in term of CC.

Fig. 5a–c illustrates the discrepancy between the anticipated and reference (experiment) values for *COD* removal, coulombic efficiency, and power predictions during the testing process of the models, including DT, SVR, FFNN, and T2FNN. Analysing the outcomes depicted in Fig. 5a, it becomes evident that the MSE between the predicted and experimental *COD* removal, as determined by the investigated DT, SVR, FFNN, and T2FNN, equates to 224.2081, 141.4224, 122.8929, and 60.7736 (%), respectively. Similarly, in the ensuing analysis, the MSE about the anticipated and experimental coulombic efficiency, facilitated by the DT, SVR, FFNN, and T2FNN models, computes to 12.5181, 8.8310, 14.3016, and 2.7720 (As), respectively, as reflected in Fig. 5b. Also, Fig. 5c shows that the MSE about the predicted and experimental power are 4.2183 $\times$ 10^3, 18.384.2183 $\times$ 10^3, 4.9056 $\times$ 10^3, and 3.0866 $\times$ 10^3 (mW/m^2) using DT, SVR, FFNN, and T2FNN.

The RMSE, gauged between the predicted and experimentally recorded *COD* removal, using DT, SVR, FFNN, and T2FNN, are 14.9736, 11.8921, 11.0857, and 7.7957 (%), respectively, following the data portrayed in Fig. 5a. Moreover, the RMSE values measured between the predicted and experimentally recorded coulombic efficiency for DT, SVR, FFNN, and T2FNN are 3.5381, 2.9717, 3.7817, and 1.6649 (As), respectively, as shown in Fig. 5b. Furthermore, as depicted in Fig. 5c, the RMSE values between the predicted and experimentally observed power are 64.9481 (mW/m^2) for DT, 135.5858 (mW/m^2) for SVR, 70.0403 (mW/m^2) for FFNN, and 55.5572 (mW/m^2) for T2FNN.

In summary, the higher accuracy of our newly proposed T2FNN compared to those of DT, SVR, and FFNN is obvious in terms of lower MSE and RMSE in predicting *COD* removal, coulombic efficiency, and

Table 2
The extracted results for investigation of implementing COD-T2FNN, CE-T2FNN and P-T2FNN for calculation of *COD* removal (%), coulombic efficiency (As), and power (mW/m^2) based on glucose(g/L), yeast extract(g/L), and aeration(mL/min).

Output	Stage	Stage	CC	MSE	Mean	Std
COD Removal	DT	Train	**0.9598**	**20.7580**	**1.4534e−15**	**4.5822**
		Test	0.7561	224.2081	5.1689	14.2470
	SVR	Train	0.8597	113.7815	0.1286	10.7272
		Test	0.7658	141.4224	−2.2541	11.8376
	FFNN	Train	0.9817	9.5620	0.0267	3.1099
		Test	0.8648	122.8929	2.7351	10.8912
	T2FNN	Train	0.9517	24.9924	0.2140	5.0233
		Test	**0.9412**	**60.7736**	**3.2902**	**7.1649**
Coulombic Efficiency	DT	Train	0.9435	2.4951	**−2.0186e−17**	1.5886
		Test	0.7451	12.5181	0.9850	3.4451
	SVR	Train	0.8142	9.7556	0.5302	3.0957
		Test	0.7868	8.8310	**0.0267**	3.0126
	FFNN	Train	0.9726	1.2314	0.0149	**1.1159**
		Test	0.7343	14.3016	0.0695	3.8333
	T2FNN	Train	**0.9728**	**1.2810**	−0.0140	1.1382
		Test	**0.9453**	**2.7720**	0.4470	**1.6259**
Power	DT	Train	0.9909	1.0113e+03	−2.1639e−14	31.9828
		Test	0.9677	4.2183e+03	10.4214	64.9909
	SVR	Train	0.9564	1.8310e+04	36.7706	130.9702
		Test	0.9462	1.8384e+04	7.1329	137.2657
	FFNN	Train	**0.9976**	**266.6385**	0.0781	**16.4225**
		Test	0.9643	4.9056e+03	**−3.8567**	70.8987
	T2FNN	Train	0.9939	4.6050e+03	25.1986	63.3693
		Test	**0.9804**	**3.0866e+03**	19.3054	**52.8137**

The bold numbers reveal the highest accurat model.

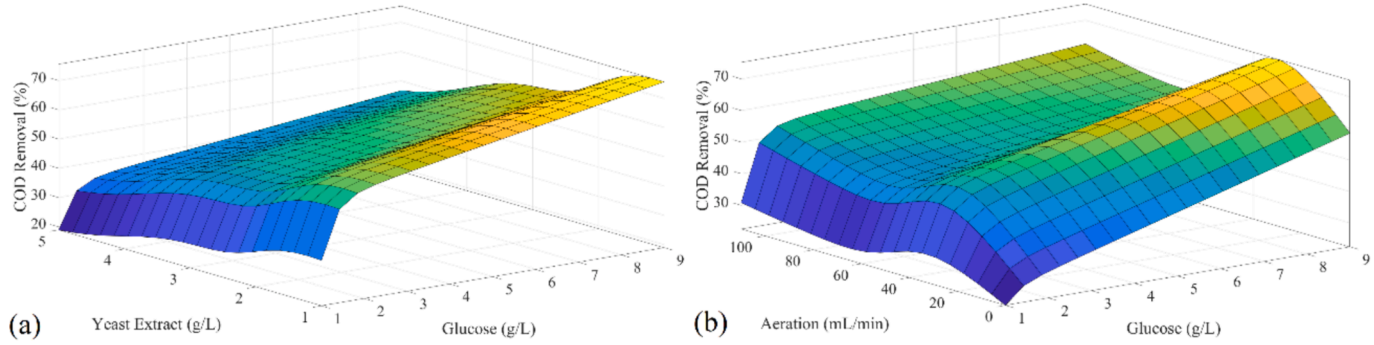

Fig. 7. COD-T2FNN rule surface for calculation of *COD* removal (%) using (a) glucose (g/L) and yeast extract (g/L); (b) glucose (g/L) and aeration (mL/min).

power.

As T2FNN is the most accurate model among the four investigated methods in this research, the linear regression plot is represented in Fig. 6a–c during the training and testing process of COD-T2FNN, CE-T2FNN and P-T2FNN for calculation of *COD* removal, coulombic efficiency, and power, respectively. As indicated in Fig. 6a, the predictive performance of COD-T2FNN in estimating *COD* removal exhibits R of 0.9517 and 0.9412 for the training and testing dataset, respectively. Similarly, Fig. 6b illustrates a distinct pattern, where R for CE-T2FNN in the domain of coulombic efficiency prediction is 0.9728 and 0.9453 for

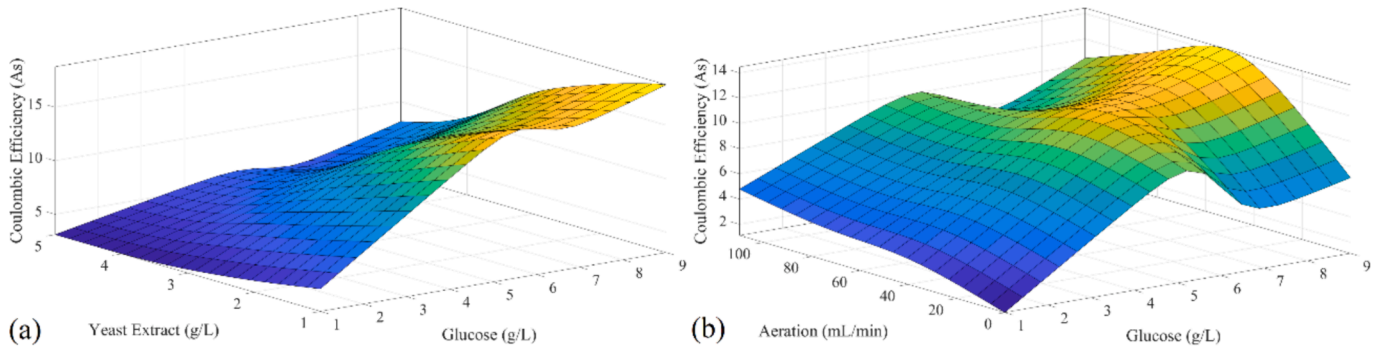

Fig. 8. CE-T2FNN rule surface for calculation of coulombic efficiency (As) using (a) glucose (g/L) and yeast extract (g/L); (b) glucose (g/L) and aeration (mL/min).

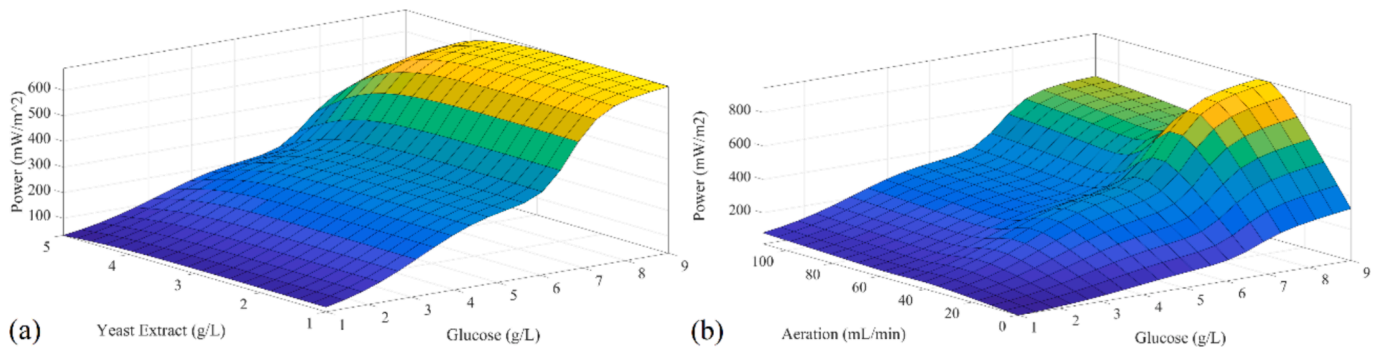

Fig. 9. P-T2FNN rule surface for calculation of power (mW/m^2) using (a) glucose (g/L) and yeast extract (g/L); (b) glucose (g/L) and aeration (mL/min).

the training and testing datasets, respectively. Also, Fig. 6c shows that the R between the experimentally captured and predicted power using P-T2FNN for training and testing datasets are 0.9804 and 0.9639, respectively.

All the represented results on Figs. 4–6 are shown in Table 2 for a quick check of the performance of the proposed methods. The concepts of MSE, CC, mean of error and standard deviation of error are used to show the efficiency of the proposed method.

Regarding computational efficiency, the training durations for COD-T2FNN, CE-T2FNN and P-T2FNN, executed on a computer equipped with Intel(R) Core(TM) i7-10875H CPU @ 2.30 GHz 2.30 GHz, amount to 6.593536, 8.702862 and 0.646226 s, respectively.

4.2. Influence of parameters

Fig. 7a–b shows the rule surface of the extracted COD-T2FNN in calculating the *COD* removal based on arrangements of the input process parameters, including glucose-yeast extract and glucose-aeration, respectively. Fig. 7a–b shows that glucose has the most influence on the variation of *COD* removal. Also, yeast extract and aeration stand in the second and third levels of influence in the variation of the *COD* removal. Based on the represented results in Fig. 7a–b, the enhancement of glucose increases *COD* removal, which is suitable for the microbial fuel cell process. In addition, the same fluence is witnessed for yeast extract based on the represented result in Fig. 7a with a lower slope. Also, the influence of aeration variation on *COD* removal is captured in Fig. 7b, which has an optimal point based on the arrangement of glucose and extract. It should be extracted via the optimisation process, which is the objective of the next subsection.

Figs. 8a–b shows the rule surface of the extracted CE-T2FNN in calculating the coulombic efficiency based on arrangements of the input process parameters, including glucose-yeast extract and glucose-aeration, respectively. Glucose has the most influence on the variation of coulombic efficiency, as shown in Fig. 8a–b. Yeast extract stands in the second level of influence in the variation of coulombic efficiency based on the results represented in Fig. 8a. It should be noted that there is no optimum point in the case of constant aeration for glucose and yeast extract. The higher coulombic efficiency is accessible with increasing the glucose and yeast extract in the case of constant aeration based on the represented results in Fig. 8a. However, the variation of aeration changes the behaviour of the system based on the represented results in Fig. 8b by elaboration of optimum point for both input parameters, including glucose and aeration. It proves the necessity of implementing the multiple-objective optimisation technique in this field to extract the optimal solution.

Fig. 9a–b shows the rule surface of the extracted P-T2FNN in calculating the power based on arrangements of the input process parameters, including glucose-yeast extract and glucose-aeration, respectively. Glucose influences the power variation most, as evidenced in Fig. 9a–b. Yeast extract and aeration stand in the second level of influence in the coulombic efficiency variation based on the results in Fig. 9ab. It should be noted that there is no optimum for glucose and yeast extract. The higher power is generated by increasing the glucose and yeast extract based on the represented results in Fig. 9a. However, there is an optimum point for aeration based on the arrangement of glucose and Yeast extract, which should be extracted using the optimisation technique.

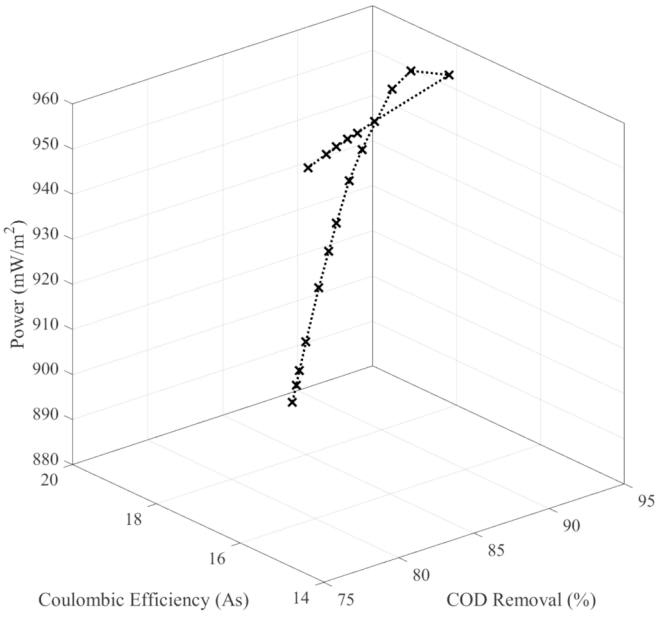

Fig. 10. Pareto front of the extracted optimal solution using multiple-objective PSO in the microbial fuel cell process to extract the *COD* removal (%), coulombic efficiency (As), and power (mW/m^2).

4.3. Optimisation

The three extracted models (COD-T2FNN, CE-T2FNN and P-T2FNN) are the objective functions of the multiple-objectives' optimisation using PSO, investigated in Eq. (13). As mentioned before, the provided toolbox by Víctor Martínez-Cagigal [37] is used for the implementation purpose of this study.

Illustrated in Fig. 10 is the distribution of the optimal solution's three-dimensional Pareto front configuration within the context of the process. Moreover, the optimal solutions derived are outlined in Table 3. A sequence of microbial fuel cell experiments was conducted to affirm the system's precision using the extracted optimal solution from the recently introduced approach. The margin of error between the experiment and predicted values of 18 optimal recommended solutions via investigated T2FNN methods are 7.41 %, 18.65 %, and 2.45 % on average for *COD* removal, coulombic efficiency, and power. This proves

Table 3
Extracted optimal process parameters of the microbial fuel cell process using T2FNN models and multiple-objective PSO.

No.	G	YE	A	COD Exp	COD Pre	COD Error	CE Exp	CE Pre	CE Error	P Exp	P Pre	P Error
1	8.99	1.01	44.49	81.2	87.00	7.15 %	16.3	19.05	16.87 %	849	884.84	4.22 %
2	8.99	1.01	44.30	80.5	87.22	8.34 %	16	19.04	19.00 %	853	888.42	4.15 %
3	8.99	1.01	44.13	79.8	87.41	9.54 %	15.5	19.03	22.77 %	866	891.56	2.95 %
4	8.99	1.01	43.81	79.9	87.79	9.88 %	15.4	19.01	23.44 %	872	897.51	2.93 %
5	9.00	1.02	43.14	77.9	88.56	13.68 %	16	18.98	18.63 %	888	908.91	2.35 %
6	9.00	1.02	42.66	76.6	89.10	16.31 %	15.6	18.94	21.41 %	889	916.51	3.09 %
7	8.99	1.02	42.22	76.4	89.52	17.17 %	14.2	18.90	33.10 %	895	922.45	3.07 %
8	8.99	1.01	41.54	86.8	90.24	3.96 %	14	18.86	34.71 %	902	931.27	3.25 %
9	8.99	1.03	40.93	85.6	90.86	6.15 %	14.6	18.78	28.63 %	915	937.90	2.50 %
10	8.98	1.02	39.18	84.2	92.40	9.73 %	16.2	18.61	14.88 %	925	950.30	2.74 %
11	9.00	1.04	38.20	87.9	93.27	6.11 %	16	18.47	15.44 %	934	954.02	2.14 %
12	9.00	1.20	36.47	88.8	94.46	6.37	16.9	17.99	6.45 %	939	953.93	1.59 %
13	9.00	1.90	37.72	82.8	85.74	3.55	17.7	16.64	**5.99 %**	942	959.05	1.81 %
14	8.99	1.92	38.66	83.2	84.83	1.96 %	18.2	16.72	8.13 %	944	957.09	1.39 %
15	9.00	2.031	37.59	80.3	83.05	3.42 %	18.6	16.32	12.26 %	948	959.47	1.21 %
16	9.00	2.08	37.58	76.8	81.95	6.70 %	19.3	16.19	16.11 %	939	959.52	2.19 %
17	9.00	2.13	37.53	78.5	80.91	3.07 %	19.44	16.06	17.39 %	943	959.56	1.76 %
18	9.00	2.23	37.49	78.8	79.01	**0.27 %**	19.9	15.81	20.55 %	952	959.75	**0.81 %**

G: glucose; YE: yeast extract; A: aeration rate; Exp: Experiment; Pre: Prediction; COD: chemical oxygen demand; CE: coulombic efficiency; P: power.
The bold numbers reveal the highest accurat model.

that P-T2FNN has the most prediction power, while CE-T2FNN is the least accurate of the three proposed T2FNN models. In addition, the lowest margin error for COD-T2FNN, CE-T2FNN and P-T2FNN are captured during the 18, 13, and 18 sets of the optimal solution with 0.27 %, 5.99 %, and 0.81 %, respectively.

5. Conclusion

Microbial fuel cells present a promising solution for renewable energy generation while simultaneously treating wastewater. This study had two primary objectives: first, to develop a surrogate model that accurately predicts microbial fuel cell performance in terms of *COD* removal, coulombic efficiency, and power output based on operational parameters such as glucose, yeast extract, and aeration; and second, to identify optimal input parameter values to maximize system performance. The main contribution of this study is developing and applying a novel methodology that integrates Type-2 Fuzzy Neural Networks (T2FNN) with multi-objective Particle Swarm Optimization (PSO). This approach begins with a comprehensive experimental investigation using a full factorial design to assess the impact of various input parameters on critical outcomes. Three distinct T2FNN models were developed to predict *COD* removal, coulombic efficiency, and power output. These models were then integrated into a multi-objective PSO framework to extract the optimal Pareto front solutions. The optimized solutions achieved a *COD* removal efficiency with a margin error of 7.41 % compared to practical investigations. The best solutions for coulombic efficiency had a margin error of 18.65 %, and the power generation optimization resulted in a margin error of 2.45 %. The proposed T2FNN models demonstrated superior performance to traditional machine learning models, highlighting their ability to handle uncertainty and variability in the data. The methodology effectively optimized the microbial fuel cell performance, showing significant improvements over previous studies and demonstrating the practical applicability of the model. To further enhance microbial fuel cell optimization, future studies could focus on expanding input parameters such as temperature, pH, and different microbial communities to develop more comprehensive models. Long-term studies are also recommended to evaluate the stability and durability of the optimized microbial fuel cell systems under real-world conditions.

Additionally, exploring the integration of microbial fuel cells with other renewable energy technologies and wastewater treatment processes to create hybrid systems could lead to improved efficiency and sustainability. Applying other advanced optimization algorithms, such as genetic or differential evolution, could further enhance the optimization process. This study's systematic approach provides a robust framework for optimizing microbial fuel cell performance, with significant implications for biotechnology and renewable energy applications. By employing T2FNN and multi-objective PSO, this research marks the first instance of media optimization in microbial fuel cells validated through experimental results, paving the way for future innovations in the field.

CRediT authorship contribution statement

Mohammad Reza Chalak Qazani: Writing – review & editing, Writing – original draft, Visualization, Validation, Supervision, Software, Resources, Project administration, Methodology, Investigation, Funding acquisition, Formal analysis, Data curation, Conceptualization. **Mostafa Ghasemi:** Writing – review & editing, Writing – original draft, Supervision, Resources, Project administration, Investigation, Funding acquisition, Formal analysis, Data curation, Conceptualization. **Houshyar Asadi:** Writing – review & editing, Writing – original draft, Project administration, Conceptualization.

Declaration of competing interest

The authors declare that they have no known competing financial interests or personal relationships that could have appeared to influence the work reported in this paper.

Data availability

Data will be made available on request.

Appendix A. Supplementary material

Supplementary data to this article can be found online at https://doi.org/10.1016/j.fuel.2024.132090.

References

[1] Ishaq H, Dincer I, Crawford C. A review on hydrogen production and utilization: challenges and opportunities. Int J Hydrogen Energy 2022;47(62):26238–64.
[2] Erenler SA, et al. Development of microbial chondroitin sulfate-based proton exchange membranes for microbial fuel cells. Fuel 2024;363:130976.
[3] Hamedani EA, Abasalt A, Talebi S. Application of microbial fuel cells in wastewater treatment and green energy production: a comprehensive review of technology fundamentals and challenges. Fuel 2024;370:131855.

[4] Elahi E, Khalid Z, Zhang Z. Understanding farmers' intention and willingness to install renewable energy technology: a solution to reduce the environmental emissions of agriculture. Appl Energy 2022;309:118459.
[5] Daud SM, et al. A critical review of ceramic microbial fuel cell: economics, long-term operation, scale-up, performances and challenges. Fuel 2024;365:131150.
[6] Tang RCO, et al. Effect of bluff body embedded in flow channel on power performance of microbial fuel cell. Fuel 2024;359:130370.
[7] Steffen B, Patt A. A historical turning point? Early evidence on how the Russia-Ukraine war changes public support for clean energy policies. Energy Res Soc Sci 2022;91:102758.
[8] Arun J, et al. New insights into microbial electrolysis cells (MEC) and microbial fuel cells (MFC) for simultaneous wastewater treatment and green fuel (hydrogen) generation. Fuel 2024;355:129530.
[9] Noor NNM, Oktavitri NI, Kim K. Effect of submerged and floating cathodes on sustainable bioelectricity generation and benthic nutrient removal in sediment microbial fuel cells. Fuel 2024;367:131438.
[10] Wang H, et al. Degradation of pyrene using single-chamber air-cathode microbial fuel cells: electrochemical parameters and bacterial community changes. Sci Total Environ 2022;804:150153.
[11] Tao M, et al. Denitrification performance, bioelectricity generation and microbial response in microbial fuel cell–constructed wetland treating carbon constraint wastewater. Bioresour Technol 2022;363:127902.
[12] Sharafat I, et al. Trivalent iron shaped the microbial community structure to enhance the electrochemical performance of microbial fuel cells inoculated with soil and sediment. J Environ Chem Eng 2022;10(3):107790.
[13] Li J, et al. Fuel properties of hydrochar and pyrochar: prediction and exploration with machine learning. Appl Energy 2020;269:115166.
[14] An H, et al. A machine learning framework for intelligent prediction of ash fusion temperature characteristics. Fuel 2024;362:130799.
[15] Agrawal P, Gnanaprakash R, Dhawane SH. Prediction of biodiesel yield employing machine learning: interpretability analysis via Shapley additive explanations. Fuel 2024;359:130516.
[16] Fang F, et al. Optimizing multi-variables of microbial fuel cell for electricity generation with an integrated modeling and experimental approach. Appl Energy 2013;110:98–103.
[17] Garg A, et al. Performance evaluation of microbial fuel cell by artificial intelligence methods. Expert Syst Appl 2014;41(4):1389–99.
[18] Chen K, Laghrouche S, Djerdir A. Degradation model of proton exchange membrane fuel cell based on a novel hybrid method. Appl Energy 2019;252:113439.
[19] Cai W, et al. Incorporating microbial community data with machine learning techniques to predict feed substrates in microbial fuel cells. Biosens Bioelectron 2019;133:64–71.
[20] Yewale A, Methekar R, Agrawal S. Multiple model-based control of multi variable continuous microbial fuel cell (CMFC) using machine learning approaches. Comput Chem Eng 2020;140:106884.
[21] Dwivedi KA, Huang S-J, Wang C-T. Integration of various technology-based approaches for enhancing the performance of microbial fuel cell technology: a review. Chemosphere 2022;287:132248.
[22] Jadhav DA, et al. Modeling and optimization strategies towards performance enhancement of microbial fuel cells. Bioresour Technol 2021;320:124256.
[23] Nguyen DD, et al. Deep learning–based optimization of a microfluidic membraneless fuel cell for maximum power density via data-driven three-dimensional multiphysics simulation. Bioresour Technol 2022;348:126794.
[24] Ghasemi M, et al. Analysis and prediction of microbial fuel cell behaviour using MLP and SVR. J Taiwan Inst Chem Eng 2023;151:105101.
[25] Ghasemi M, Rezk H. Performance improvement of microbial fuel cell using experimental investigation and fuzzy modelling. Energy 2023:129486.
[26] Abdollahfard Y, Sedighi M, Ghasemi M. A new approach for improving microbial fuel cell performance using artificial intelligence. Sustainability 2023;15(2):1312.
[27] Nguyen DD, et al. Guiding the optimization of membraneless microfluidic fuel cells via explainable artificial intelligence: comparative analyses of multiple machine learning models and investigation of key operating parameters. Fuel 2023;349:128742.
[28] Hossain SZ, et al. Modeling of microbial fuel cell power generation using machine learning-based super learner algorithms. Fuel 2023;349:128646.
[29] Kebede GA, et al. Transfer learning-based deep learning models for proton exchange membrane fuel remaining useful life prediction. Fuel 2024;367:131461.
[30] Li H-W, et al. Maximizing power density in proton exchange membrane fuel cells: an integrated optimization framework coupling multi-physics structure models, machine learning, and improved gray wolf optimizer. Fuel 2024;358:130351.
[31] Ghasemi M, et al. Performance improvement of microbial fuel cell through artificial intelligence. Int J Energy Res 2021;45(1):342–54.
[32] Mohammadi M, et al. Microbial fuel cell for oilfield produced water treatment and reuse: modelling and process optimization. Korean J Chem Eng 2021;38:72–80.
[33] Lin Y-Y, et al. Simplified interval type-2 fuzzy neural networks. IEEE Trans Neural Netw Learn Syst 2013;25(5):959–69.
[34] Mendel JM. Advances in type-2 fuzzy sets and systems. Inf Sci 2007;177(1):84–110.
[35] Kennedy J, Eberhart R. Particle swarm optimization. In: Proceedings of ICNN'95-international conference on neural networks. IEEE; 1995.
[36] Coello CAC, Pulido GT, Lechuga MS. Handling multiple objectives with particle swarm optimization. IEEE Trans Evol Comput 2004;8(3):256–79.
[37] Martínez-Cagigal V. Multi-objective particle swarm optimization (MOPSO); 2023. Available from: https://es.mathworks.com/matlabcentral/fileexchange/62074-multi-objective-particle-swarm-optimization-mopso?s_tid=FX_rc3_behav.